CONF-761138--2

DYNAMICS OF A CYLINDRICAL SHELL SYSTEM COUPLED BY VISCOUS FLUID

T. T. Yeh and S. S. Chen

Ninety-second Meeting of
Acoustical Society of America
San Diego, California
November 16-19, 1976

UofC-AUA-USERDA

ARGONNE NATIONAL LABORATORY, ARGONNE, ILLINOIS

operated under contract W-31-109-Eng-38 for the
U. S. ENERGY RESEARCH AND DEVELOPMENT ADMINISTRATION

DYNAMICS OF A CYLINDRICAL SHELL SYSTEM COUPLED BY VISCOUS FLUID*

T. T. Yeh and S. S. Chen

Components Technology Division

Argonne National Laboratory

9700 S. Cass Avenue

Argonne, Illinois 60439

SEPTEMBER 1976

---

*To be presented at the Ninety-second Meeting of the Acoustical Society of America, November 16-19, 1976 at San Diego, California.

ABSTRACT

This study was motivated by the need to design the thermal shield in reactor internals and other system components to avoid detrimental flow-induced vibrations. The system component is modeled as two coaxial shells separated by a viscous fluid. In the analysis, Flügge's shell equations of motion and linearized Navier-Stokes equation for viscous fluid are employed. First, a traveling-wave type solution is taken for shells and fluid. Then, from the interface conditions between the shells and fluid, the solution for the fluid medium is expressed in terms of shell displacements. Finally, using the shell equations of motion gives the frequency equation, from which the natural frequency, mode shape, and modal damping ratio of coupled modes can be calculated. The analytical results show a fairly good qualitative agreement with the published experimental data. With the presented analysis and results, the frequency and damping characteristics can be analyzed and design parameters can be related to frequency and damping.

INTRODUCTION

In this paper, the dynamics of a system of two concentric cylindrical shells coupled by a viscous fluid is studied analytically. The objective is to investigate the effect of fluid viscosity on fluid structure interactions.

This study was motivated by the need to design reactor system components to avoid detrimental flow-induced vibrations. Several reactor system components consist of nominally circular cylindrical shells coupled to other shells through a fluid. Examples include shrouds and thermal liners. Those components are subject to various excitation sources including fluid flow and structural borne disturbance. To design a component such that over the design life its performance will not be affected by vibrations, one must understand the system characteristics.

Vibrations of two coaxial shells separated by a fluid have been studied recently [1-4]. However, all those investigations omit the effect of fluid viscosity. Although for many practical applications, the viscosity is small and the fluid may be considered inviscid as a first approximation, near the interface of the structure and fluid there exists a thin layer of rotational flow. This flow regime in which the viscous effect is significant is of great concern to the dynamic response of coupled shell systems. In particular, when the annular gap is small, the fluid viscous effect becomes more pronounced.

In this study, Flügge's shell equations of motion and the linearized Navier-Stokes equation for fluid are employed. First, a traveling-wave type solution is taken for shells and fluid. Then, from the interface conditions between the shells and fluid, the solution for fluid medium

is expressed in terms of shell displacements. Finally, using the shell equations of motion gives the frequency equation from which the natural frequency, mode shape, and the modal damping ratio can be calculated. The analytical results are also compared with an experimental investigation for two concentric shells coupled by water.

I. GOVERNING EQUATIONS OF MOTION

Consider two concentric circular cylindrical shells separated by a viscous fluid annulus as shown in Fig. 1. The motion of the shells is described by the following Flügge's shell equation [5]:

$$\left[\frac{\partial^2}{\partial z^2} + \left(\frac{1-\nu_i}{2R_i^2}\right)\left(1+\frac{h_i^2}{12\,R_i^2}\right)\frac{\partial^2}{\partial\theta^2}\right] u_i + \frac{1+\nu_i}{2\,R_i}\frac{\partial^2 v_i}{\partial z\partial\theta}$$

$$+ \left[\frac{\nu_i}{R_i}\frac{\partial}{\partial z} - \frac{h_i^2}{12\,R_i}\frac{\partial^3}{\partial z^3} + \frac{(1-\nu_i)h_i^2}{24\,R_i^3}\frac{\partial^3}{\partial z\partial\theta^2}\right] w_i$$

$$= \frac{\rho_i(1-\nu_i^2)}{E_i}\frac{\partial^2 u_i}{\partial t^2} - \frac{1-\nu_i}{E_i\,h_i} P_{zi} ;$$

$$\frac{1+\nu_i}{2R_i}\frac{\partial^2 u_i}{\partial z\partial\theta} + \left[\frac{1}{R_i^2}\frac{\partial^2}{\partial\theta^2} + \frac{1-\nu_i}{2}\left(1+\frac{h_i^2}{4\,R_i^2}\right)\frac{\partial^2}{\partial z^2}\right] v_i \tag{1}$$

$$+ \left[\frac{1}{R_i^2}\frac{\partial}{\partial\theta} - \frac{(3-\nu_i)h_i^2}{24R_i^2}\frac{\partial^3}{\partial\theta\partial z^2}\right] w_i = \frac{\rho_i(1-\nu_i^2)}{E_i}\frac{\partial^2 v_i}{\partial t^2}$$

$$- \frac{1-\nu_i^2}{E_i\,h_i} P_{\theta i} ;$$

$$\left[-\frac{h_i^2}{12\,R_i}\frac{\partial^3}{\partial z^3} + \frac{\nu_i}{R_i}\frac{\partial}{\partial z} + \frac{(1-\nu_i)h_i^2}{24\,R_i^3}\frac{\partial^3}{\partial z\,\partial\theta^2}\right] u_i$$

$$+ \left[-\frac{(3-\nu_i)h_i^2}{24\,R_i^2}\frac{\partial^3}{\partial\theta\partial z^2} + \frac{1}{R_i^2}\frac{\partial}{\partial\theta}\right] v_i$$

$$+\left[\frac{1}{R_i^2}+\frac{h_i^2}{12R_i^4}+\frac{h_i^2}{12}\frac{\partial^4}{\partial z^4}+\frac{h_i^2}{6R_i^2}\frac{\partial^4}{\partial z^2\partial\theta^2}+\frac{h_i^2}{12R_i^4}\frac{\partial^4}{\partial\theta^4}+\frac{h_i^2}{6R_i^4}\frac{\partial^2}{\partial\theta^2}\right]w_i$$

$$=-\frac{\rho_i(1-\nu_i^2)}{E_i}\frac{\partial^2 w_i}{\partial t^2}+\frac{1-\nu_i^2}{E_i h_i}P_{ri}\ ; \qquad (1)\ \text{(Contd.)}$$

where the index i denotes the variables associated with the inner shell (i = 1) and outer shell (i = 2); u_i, v_i, w_i are the displacement components of the shell middle surfaces, z, θ, and r are cylindrical coordinates; P_{zi}, $P_{\theta i}$, and P_{ri} are the surface loading components per unit area, and t is the time. The physical characteristics of shells are defined by the mean radius R_i, wall thickness h_i, mass density ρ_i, Young's modulus E_i and Poisson's ratio ν_i.

For a non-steady, small-amplitude oscillatory motion, the equations of motion for the contained viscous fluid can be expressed as follows [6]:

$$\left.\begin{aligned}&\frac{\partial\rho}{\partial t}+\rho_o\ \nabla\cdot\vec{V}=0\ ,\\ &\frac{\partial\vec{V}}{\partial t}=-\frac{1}{\rho_o}\nabla p+\left(\frac{4}{3}\nu_o+\nu_o'\right)\nabla(\nabla\cdot\vec{V})-\nu_o\ \nabla\times\nabla\times\vec{V}\ ,\\ &\frac{\partial p}{\partial\rho}=C_o^2\ ,\end{aligned}\right\} \qquad (2)$$

where ρ_o and ρ are the mean and instantaneous fluid mass densities, ν_o and ν_o' are the kinematic and second viscosities of the fluid, C_o is the speed of sound in fluid, p is fluid pressure and $\vec{V}$ is fluid velocity vector.

At the interfaces between the shells and fluid, the following conditions must be satisfied:

$$V_z\Big|_{r=r_i} = \frac{\partial u_i}{\partial t} \; ; \quad V_\theta\Big|_{r=r_i} = \frac{\partial v_i}{\partial t} \; ; \text{ and } V_r\Big|_{r=r_i} = \frac{\partial w_i}{\partial t} \text{ with } i = 1 \text{ and } 2. \tag{3}$$

The surface loading acting on the shells is given by

$$P_{\ell 1} = \tau_{r\ell}\Big|_{r=r_1} \text{ and } P_{\ell 2} = -\tau_{r\ell}\Big|_{r=r_2} \text{ with } \ell = z,\theta, \text{ and } r, \tag{4}$$

where $r_1 = R_1 + h_1/2$ and $r_2 = R_2 - h_2/2$ are the interface radii, and τ_{rr}, $\tau_{r\theta}$, and τ_{rz} are the fluid stresses:

$$\begin{aligned} \tau_{rr} &= -p + 2\,\mu\,\frac{\partial V_r}{\partial r} \; , \\ \tau_{r\theta} &= \mu\left[r\,\frac{\partial}{\partial r}\left(\frac{V_\theta}{r}\right) + \frac{1}{r}\,\frac{\partial V_r}{\partial \theta}\right] \; , \\ \tau_{rz} &= \mu\left(\frac{\partial V_r}{\partial z} + \frac{\partial V_z}{\partial r}\right) \; . \end{aligned} \tag{5}$$

Here μ is fluid viscosity.

Equations (1) through (5) are the complete mathematical statement of the coupled viscous fluid/shell system.

II. ANALYSIS

Letting $\vec{V} = \nabla \times \vec{\psi} + \nabla\phi$ and inserting it into equations (2) yields

$$(\frac{\partial}{\partial t} - \nu_o \nabla^2)\vec{\psi} = 0, \tag{6}$$

$$p = p_o - \rho_o \frac{\partial\phi}{\partial t} + \rho_o(\frac{4\nu_o}{3} + \nu_o')\nabla^2\phi \quad , \tag{7}$$

$$[(1 + \frac{1}{\omega_o}\frac{\partial}{\partial t})\nabla^2 - \frac{1}{C_o^2}\frac{\partial^2}{\partial t^2}]\phi = 0 \quad , \tag{8}$$

where

$$\omega_o = C_o^2/(\frac{4}{3}\nu_o + \nu_o') \quad .$$

Equation (7) shows that the fluid pressure is not affected by the waves produced from the vector potential, $\vec{\psi}$, which is associated with the fluid viscosity.

In cylindrical coordinates, equation (6) yields:

$$(\frac{1}{\nu_o}\frac{\partial}{\partial t} - \nabla^2)\psi_z = 0 \quad ,$$

$$(\frac{1}{\nu_o}\frac{\partial}{\partial t} - \nabla^2)\psi_\theta + \frac{\psi_\theta}{r^2} - \frac{2}{r^2}\frac{\partial\psi_r}{\partial\theta} = 0, \tag{9}$$

and

$$(\frac{1}{\nu_o}\frac{\partial}{\partial t} - \nabla^2)\psi_r + \frac{\psi_r}{r^2} + \frac{2}{r^2}\frac{\partial\psi_\theta}{\partial\theta} = 0 \quad .$$

Solutions of the following form are assumed for the shells:

$$\begin{aligned} u_i &= j\ \bar{u}_i \cos(n\ \theta)\ \exp[j(\omega t - kz)] \quad , \\ v_i &= \bar{v}_i\ \sin(n\ \theta)\ \exp[j(\omega t - kz)] \quad , \\ w_i &= \bar{w}_i \cos(n\ \theta)\ \exp[j(\omega t - kz)] \quad , \end{aligned} \tag{10}$$

where $j = \sqrt{-1}$, n is the circumferential wave number, ω is the circular frequency, k is the axial wave number, and $\bar{u}_i$, $\bar{v}_i$ and $\bar{w}_i$ are arbitrary constants to be determined.

Similarly, the fluid velocity potential may be assumed as follows:

$$\begin{aligned} \phi &= \bar{\phi}(r) \cos n\theta \exp[j(\omega t - kz)] , \\ \psi_z &= \bar{\psi}_z(r) \sin n\theta \exp[j(\omega t - kz)] , \\ \psi_\theta &= j\,\bar{\psi}_\theta(r) \cos n\theta \exp[j(\omega t - kz)] , \\ \psi_r &= j\,\bar{\psi}_r(r) \sin n\theta \exp[j(\omega t - kz)] . \end{aligned} \tag{11}$$

Substituting Eqs. (11) into (8) and (9) gives the following forms of Bessel's equations:

$$\left.\begin{aligned} &\left[\frac{1}{r}\frac{\partial}{\partial r}\left(r\frac{\partial}{\partial r}\right) + \left(k_1^2 - \frac{n^2}{r^2}\right)\right]\bar{\phi} = 0 , \\ &\left[\frac{1}{r}\frac{\partial}{\partial r}\left(r\frac{\partial}{\partial r}\right) + \left(k_2^2 - \frac{n^2}{r^2}\right)\right]\bar{\psi}_z = 0 , \\ &\frac{1}{r}\frac{\partial}{\partial r}\left(r\frac{\partial}{\partial r}\bar{\psi}_\theta\right) + \left(k_2^2 - \frac{n^2+1}{r^2}\right)\bar{\psi}_\theta + \frac{2n}{r^2}\bar{\psi}_r = 0 , \\ &\frac{1}{r}\frac{\partial}{\partial r}\left(r\frac{\partial}{\partial r}\bar{\psi}_r\right) + \left(k_2^2 - \frac{n^2+1}{r^2}\right)\bar{\psi}_r + \frac{2n}{r^2}\bar{\psi}_\theta = 0 , \end{aligned}\right\} \tag{12}$$

where

$$\left.\begin{aligned} k_1 &= \left(-k^2 + \frac{\omega^2/C_o^2}{1 + j\frac{\omega}{\omega_o}}\right)^{1/2} , \\ k_2 &= \left(-k^2 - j\frac{\omega}{\nu_o}\right)^{1/2} . \end{aligned}\right\} \tag{13}$$

The general solutions of equations (12) are

$$\bar{\phi}(r) = j\,\omega[A_1 F_n(k_1 r) + A_2 G_n(k_1 r)] \quad ,$$

$$\bar{\psi}_z(r) = j\,\omega[A_3 F_n(k_2 r) + A_4 G_n(k_2 r)] \quad , \tag{14}$$

$$\bar{\psi}_r(r) = -\bar{\psi}_\theta(r) = j\,\omega[A_5 F_{n+1}(k_2 r) + A_6 G_{n+1}(k_2 r)] \quad ,$$

where A_i are arbitrary constants and F_n and G_n are the n-th order Bessel functions. F_n and G_n can be either the first and second kind Bessel functions, J_n and Y_n, or the Hankel functions $H_n^{(1)}$ and $H_n^{(2)}$. The selection of the functions mainly depends on the computational consideration.

Substituting equations (10), (11), and (14) into the interface conditions, Eq. (3), gives six linear, algebraic equations:

$$\sum_{q=1}^{6} a_{pq} A_q = \hat{r}_p \hat{u}_p \quad , \quad p = 1 \text{ to } 6 \tag{15}$$

where

$$\hat{r}_p = r_1 \text{ for } p = 1,\ 2,\ \text{and } 3, \qquad \hat{r}_p = r_2 \text{ for } p = 4,5,6$$

$$\hat{u}_1 = \bar{u}_1,\ \ \hat{u}_2 = \bar{v}_1,\ \ \hat{u}_3 = \bar{w}_1,\ \ \hat{u}_4 = \bar{u}_2,\ \ \hat{u}_5 = \bar{v}_2,\ \text{and } \hat{u}_6 = \bar{w}_2$$

and the expression of a_{pq} is given in the appendix.

Now we are in the position to calculate the loading stresses on the shell surfaces. Here only the dynamic quantity is of interest and thus the reference pressure p_o will not be considered. Equation (5) is used to obtain the fluid stresses. Define the new variables $\bar{P}_{zi}$, $\bar{P}_{\theta i}$, and $\bar{P}_{ri}$ as follows:

$$P_{zi} = j\,\rho_o\,\omega^2\,\bar{P}_{zi}\cos(n\,\theta)\ \ \exp[j(\omega t - kz)],$$

$$P_{\theta i} = \rho_o\,\omega^2\,\bar{P}_{\theta i}\,\sin(n\,\theta)\,\exp[j(\omega t - kz)], \tag{16}$$

and

$$P_{ri} = \rho_o\,\omega^2\,\bar{P}_{ri}\,\cos(n\,\theta)\,\exp[j(\omega t - kz)] \quad .$$

Substituting equation (16) into (4) and using (11) and (14) yield another six linear, algebraic equations:

$$\sum_{q=1}^{6} h_{pq} A_q = \hat{P}_p \quad , \quad p = 1 \text{ to } 6, \tag{17}$$

where $\hat{P}_1 = \bar{P}_{z1}$, $\hat{P}_2 = \bar{P}_{\theta 1}$, $\hat{P}_3 = \bar{P}_{r1}$, $\hat{P}_4 = \bar{P}_{z2}$, $\hat{P}_5 = \bar{P}_{\theta 2}$, $\hat{P}_6 = \bar{P}_{r2}$,

and the expression of h_{pq} is given in the appendix.

Using equations (15) and (17) gives the surface loading expressed in terms of the interface radii and the shell displacement as

$$\hat{P}_p = \sum_{q=1}^{6} \alpha_{pq} \hat{r}_q \hat{u}_q, \quad p = 1 \text{ to } 6, \tag{18}$$

where

$$\{\alpha_{pq}\} = \{h_{pq}\} \{a_{pq}\}^{-1} . \tag{19}$$

The coefficient α_{pp} is proportional to the dynamic fluid stress acting on a shell surface due to its own movement; while the others, α_{pq} for $p \neq q$, are proportional to the dynamic fluid stresses acting on a shell surface in one direction due to the movement in another direction.

The fluid stresses acting on the shells are linear functions of shell motions. In general, the coefficients α_{pq} are complex. The fluid stress can be separated into two components: one proportional to $\mathrm{Re}(\alpha_{pq})$ is in phase with the shell accelerations and is related to the added mass effect, while the other, proportional to $\mathrm{Im}(\alpha_{pq})$, is opposing to the movement of the shells and is related to damping mechanism. If the fluid is inviscid, the second component of the stress opposing shell motion will be zero.

The dynamic fluid stress coefficient matrix α_{pq} is a function of the radius ratio, r_2/r_1, the circumferential wave number, n, the axial wave number, α_1, the Mach number $Mo_1 = \frac{\omega r_1}{C_o}$, the Reynolds number, $Re_1 = \frac{\omega r_1^2}{\nu_o}$, and the ratio of the fluid viscosities ν_o'/ν_o. It should be noted that the circular frequency ω and so Mach number Mo_1 and Reynolds number Re_1 are in general complex numbers. The Mach number Mo_1 is considered to include the compressibility effects of the fluid. However, the analysis is valid for a small compressible effect or a small Mach number Mo_1. The Reynolds number Re_1 and viscosity ratio ν_o'/ν_o are the additional function parameters associated with fluid viscosity. The viscous effect is discussed in detail in the study.

For the case of potential flow where $\nu_o = 0$, and $\nu_o' = 0$, the Reynolds number Re_1 and viscous ratio ν_o'/ν_o are no longer defined and the coefficient is a function of r_2/r_1, n, α_1 and Mo_1 only. Furthermore, all the elements of the coefficient matrix are zero except the real parts of the four elements: $Re\{\alpha_{33}\}$, $Re\{\alpha_{36}\}$, $Re\{\alpha_{63}\}$, and $Re\{\alpha_{66}\}$, and no damping is introduced to the system by the incompressible ideal fluid [1].

With respect to fluid shell interaction, substituting eqs. (10), (16), and (18) into the shell eq. (1) gives six linear algebraic homogeneous equations

$$\sum_{q=1}^{6} b_{pq} \hat{u}_q = 0, \quad p = 1 \text{ to } 6, \tag{20}$$

where

$$\begin{aligned}
b_{pq} &= C_{pq} - \Omega_1^2(\delta_{pq} + \mu_1\alpha_{pq}) , && \text{for p,q = 1, 2 and 3} ,\\
&= -\Omega_1^2\left(\delta_{pq} + \mu_1 \frac{r_2}{r_1}\alpha_{pq}\right) , && \text{for p = 1, 2, and 3} ,\\
& && \text{and q = 4, 5, and 6} ,\\
&= -\Omega_2^2\left(\delta_{pq} + \mu_2 \frac{r_1}{r_2}\alpha_{pq}\right) , && \text{for p = 4, 5, and 6} ,\\
& && \text{and q = 1, 2, and 3} ,\\
&= C_{pq} - \Omega_2^2(\delta_{pq} + \mu_2\alpha_{pq}) , && \text{for p,q = 4, 5, and 6} ,
\end{aligned}$$

$$\Omega_i = R_i\omega\left[\frac{\rho_i(1-\nu_i^2)}{E_i}\right]^{1/2} , \qquad \mu_i = \frac{\rho_o r_i}{\rho_i h_i} ,$$

$$\delta_{pq} = 1 \quad \text{for } p = q, \text{ otherwise } \delta_{pq} = 0 ,$$

and the expression of C_{pq} is given in the Appendix.

The frequency equation of the coupled fluid/shell system is obtained by setting the determinant of the coefficient matrix b_{pq} in equation (20) equal to zero; it can be written as $|b_{pq}| = 0$ or in the function form as

$$F(\alpha_1, r_2/r_1, Mo_1, Re_1, \nu_o'/\nu_o, n, \Omega_i, \delta_i, \mu_i) = 0 . \qquad (21)$$

In contrast with the incompressible potential flow theory, the stress coefficient for a given physical condition is a function of the frequency parameter, ω, which in general is a complex number. Therefore, in order to determine the natural frequency and the damping ratio of the coupled system, an iteration procedure is in general required.

It should be noted that, for the case of an incompressible viscous fluid, the dynamic fluid stress is not only a function of n, r_2/r_1, and α_1 but also a function of the vibrational Reynolds number Re_1. This additional parameter Re_1 makes the simulation of a scaled model test for a coupled viscous fluid/shell system to be very difficult when fluid viscosity effect is important. In a reduced-scale model test, the geometrical simulation commonly employed tends to overestimate the fluid damping and thus the test result may not be conservative.

III. NUMERICAL EXAMPLES

The preceding analysis can be used to evaluate the stress coefficient matrix, α_{pq}, for two concentric shells separated by viscous fluid for any given set of input parameters n, r_2/r_1, α_1, Mo_1, Re_1, and ν_o'/ν_o.

Some numerical examples of the stress coefficients were obtained and shown in Table 1 and Figs. 2 to 4. All examples given are for incompressible fluid ($Mo_1 = 0$), the length of both shells equal to radius r_1 ($\alpha_1 = \pi$), and $\nu_o' = 0$. Also the circular frequency ω is limited to a purely real number. That is, $Im(\omega) = Im(Re_1) = 0$.

Table 1 shows the stress coefficient matrix for $\alpha_1 = \pi$, $n = 3$, $r_2/r_1 = 1.2$ and $Mo_1 = 0$. Each element is specified by a real part (upper number) and an imaginary part (lower number). In Table 1a all the values of α_{pq} are very small except $Re\{\alpha_{33}\} = 0.324$, $Re\{\alpha_{36}\} = Re\{\alpha_{63}\} = -0.234$, and $Re\{\alpha_{66}\} = 0.318$. In this case, the Reynolds number is large ($Re_1 = 10^{10}$); as expected the imaginery part of α_{pq} is not important. The results are consistent with the solutions of the potential flow [1], which shows $\alpha_{33} = 0.324$, $\alpha_{36} = \alpha_{63} = -0.234$, $\alpha_{66} = 0.318$ and all others are zero. However, for the case of small Reynolds number, the viscous effect becomes important; the imaginary part of α_{pq} becomes more important and, in some cases, the imaginary part may be larger than the real part. This can be seen from Table 1b for $Re_1 = 10$, the imaginary parts of α_{pq} are, indeed, much larger than their real parts.

Figure 2 shows the stress coefficient α_{33} as a function of Reynolds number Re_1 as well as n for $\alpha_1 = \pi$, $r_2/r_1 = 1.1$ and $Mo_1 = 0.0$. α_{33} decreases as the Reynolds number Re_1 increases; this behavior is the same as that of a vibrating rod in confined viscous fluids [7]. For fixed values of r_1, r_2, and ν_o, $Re\{\alpha_{33}\}$ decreases with an increasing ω; this behavior is consistent with the experimental observations [8]. It is

TABLE 1. Dynamic Stress Coefficient Matrix a_{pq} for $\alpha_1 = \pi$, $n = 3$, $r_2/r_1 = 1.2$ and $Mo_1 = 0.0$.

	p \ q	1	2	3	4	5	6
$Re_1 = 10^{10}$ (a)	1	7.07E-6 -7.07E-6	0 0	-7.19E-6 7.19E-6	0 0	0 0	5.20E-6 -5.20E-6
	2	0 0	7.07E-6 -7.07E-6	-6.86E-6 6.86E-6	0 0	0 0	4.97E-6 -4.97E-6
	3	-7.19E-6 7.19E-6	6.86E-6 6.86E-6	3.24E-1 -2.15E-5	-5.20E-6 5.20E-6	-4.14E-6 4.14E-6	-2.34E-1 2.03E-5
	4	0 0	0 0	-5.20E-6 5.20E-6	5.89E-6 -5.89E-6	0 0	7.05E-6 -7.05E-6
	5	0 0	0 0	-4.14E-6 4.14E-6	0 0	5.89E-6 -5.89E-6	5.61E-6 -5.61E-6
	6	5.20E-6 -5.20E-6	4.97E-6 -4.97E-6	-2.34E-1 2.03E-5	7.05E-6 -7.05E-6	5.61E-6 -5.61E-6	3.18E-1 -2.11E-5
$Re_1 = 10$ (b)	1	4.14E-2 -1.49E 0	-1.67E-2 -7.32E-1	-2.13E-2 2.32E 0	7.46E-3 -3.33E-1	-1.59E-2 -6.21E-1	1.25E-2 -2.60E 0
	2	-1.67E-2 -7.32E-1	4.64E-2 -1.42E 0	-2.22E-2 2.03E 0	-1.61E-2 -6.64E-1	1.20E-2 -1.52E-1	1.25E-2 -2.34E 0
	3	-2.13E-2 2.32E 0	-2.22E-2 2.03E 0	3.85E-1 -9.38E 0	-1.28E-2 2.47E 0	-1.02E-2 2.06E 0	-2.91E-1 8.93E 0
	4	7.46E-3 -3.33E-1	-1.61E-2 -6.64E-1	-1.28E-2 2.47E 0	3.48E-2 -1.20E 0	-1.41E-2 -6.11E-1	2.24E-2 -2.20E 0
	5	-1.59E-2 -6.21E-1	1.20E-2 -1.52E-1	-1.02E-2 2.06E 0	-1.41E-2 -6.11E-1	3.86E-2 -9.20E-1	1.66E-2 1.89E 0
	6	1.25E-2 -2.60E 0	1.25E-2 -2.34E 0	-2.91E-1 8.93E 0	2.24E-2 -2.20E 0	1.66E-2 -1.89E 0	3.78E-1 -8.87E 0

interesting to note that the sensitivity of all $Re\{\alpha_{pq}\}$ with respect to Re_1 is much smaller than $Im\{\alpha_{pq}\}$, although both $Re\{\alpha_{pq}\}$ and $Im\{\alpha_{pq}\}$ increase with decreasing Re_1. Figure 2 also shows that both $Re\{\alpha_{33}\}$ and $Im\{-\alpha_{33}\}$ are the decreasing function of n.

Figures 3 and 4 show the stress coefficients α_{33} and α_{66} as functions of r_2/r_1, n, and Re_1 for $\alpha_1 = \pi$ and $Mo_1 = 0$. In all cases, as the values of r_2/r_1 increase, α_{33} approaches a constant value while α_{66} monotonically decreases. The different behaviors between α_{33} and α_{66} is attributed to the choice of inner radius r_1 (rather than r_2) as a reference length scale. As the value of r_2/r_1 becomes large, the movement of either shell is less dependent on the existence of the other and the stress coefficients are expected to approach a constant value if all other parameters for the shell are kept unchanged. However, the present example is set to keep α_1, Re_1, and Mo_1 unchanged, and so α_2, Re_2 and Mo_2 which are the important parameters for the outer shell are increased as r_2/r_1 increases. This means there will be a larger three-dimensional effect, a larger compressibility effect and a smaller viscous effect for the outer shell as r_2/r_1 increases, although these effects are relatively constant for the inner shell.

For $r_2/r_1 > 2.0$ the outer shell has practically no effects on α_{33} and the effect of the inner shell on the outer shell seems no longer important and the decrease of α_{66} is primarily due to the increase of α_2 or the decrease of length/radius for the outer shell. With respect to the dependence of n, both α_{33} and α_{66} decrease as n increases. Also the decreasing rate for $Re\{\alpha_{33}\}$ and $Re\{\alpha_{66}\}$ is smaller as Re_1 increases, while this behavior for $Im\{-\alpha_{33}\}$ and $Im[-\alpha_{66}]$ is more pronounced.

Note that the example given here is for $Mo_1 = 0$. For case of $Mo_1 > 0$, the value of α_{pq} is expected to be smaller. It can be concluded that the stress coefficient is a decreasing function of the parameters α_1, Mo_1, Re_1, and r_2/r_1 and in most cases it is a decreasing function of n.

For a specific numerical example of a coupled fluid/shell system, consider the following dimensional values: $R_1 = 86.52$ cm (34.0625 in.), $R_2 = 88.74$ cm (34.9375 in.), $h_1 = 0.635$ cm (0.25 in.), $h_2 = 1.5875$ cm (0.625 in.), $E_1 = E_2 = 1.896 \times 10^{11}$ Pa (2.75×10^7 psi), $\nu_1 = \nu_2 = 0.27$, $\rho_1 = \rho_2 = 7.986 \times 10^3$ kg/m^3 (0.2885 lbm/in.^{3}), $\rho_o = 9.217 \times 10^2$ kg/m^3 (0.0333 lbm/in.^{3}), $\nu_o = 7.432 \times 10^{-7}$ m^2/s (8.0×10^{-6} ft^2/sec), $\nu_o' = 0$ and $C_o = \infty$. This is the same example as that given in Ref. 1, with the exception that, in the present case, there is no fluid inside the inner shell and the fluid is viscous in the annulus region. The fluid is considered to be incompressible, $Mo_1 = 0$, and the shell is assumed to be simply supported at both ends.

The frequencies of the system depend on the axial wave number α_i and circumferential wave number n. The lowest frequency is associated with the lowest axial wave number, i.e., the wavelength is equal to twice the shell length which is assumed to be 104.14 cm (41 in.).

The natural frequencies for the cases of viscous fluid are shown in Fig. 5. For comparison, four related cases are also shown: (1) the inner shell in vacuo; (2) the outer shell in vacuo; (3) the shell system with rigid outer shell; and (4) the shell system with rigid inner shell. It can be seen from Fig. 5 that natural frequencies of the system decrease due to the existence of the fluid and for each circumferential wavenumber n the natural frequencies for the first coupled modes (out-of-phase modes)

are lower than either of the uncoupled natural frequencies, while the frequencies for the second coupled modes (in-phase modes) are higher than either of the uncoupled natural frequencies.

Calculations for an inviscid fluid are also made. It is found that these natural frequencies are practically independent of the fluid viscosity. However, as shown in Fig. 6, the related modal damping ratio is noticeably increased in some cases when the fluid viscosity is included. These results are expected since the fluid viscosity (related to Re_1) has a smaller effect on $Re\{\alpha_{pq}\}$ and has a larger effect on $Im\{\alpha_{pq}\}$. The decrease in natural frequencies is due to fluid inertia effect, which is proportional to $Re\{\alpha_{pq}\}$, while the increase in damping is mainly attributed to fluid drag, which is proportional to $Im\{\alpha_{pq}\}$.

The effects of fluid viscosity on coupled and uncoupled modes are clearly shown. For the coupled shell systems the effects are mostly pronounced for the out-of-phase modes, but these effects are much smaller and in fact are considered to be negligible for the in-phase modes. However, for the uncoupled vibrations, the effects of fluid viscosity remain comparable for both shells. The reason for large damping ratios on out-of-phase modes and small damping ratios on in-phase modes can be seen from the differences of the vibrational mode-shapes which are shown in Fig. 7. For in-phase modes, both shells as well as the fluid in the annular region are moved almost in the same way (i.e., amplitude ratios $\approx$ 1.0) and so the existence of the fluid is hardly noticed by the shells. However, for the out-of-phase modes, two shells are moved in opposite directions and the existence of the fluid is mostly detected by the shells. Also, the frequencies and so the vibrational Reynolds number Re_1 for the in-phase modes are much higher than for the out-phase modes.

Thus the modal damping is much smaller for the in-phase modes than for the out-phase modes. For $n \geq 6$ the movement of inner shell is much larger than of outer shell and the result is close to that of uncoupled shell system with rigid outer shell. For $n \leq 2$ or $n \geq 11$ the in-phase mode data were not presented because of the high natural frequencies.

Additional calculations also have been made to understand the effect of fluid compressibility. It is found that the effect of fluid compressibility, in general, is very small on natural frequency and damping, and in practical applications for structural vibrations, the compressibility of the fluid may be neglected. On the other hand, if the propagation of waves in the system is of interest, fluid compressibility has to be included.

IV. COMPARISON OF ANALYTICAL AND EXPERIMENTAL RESULTS

An experimental study on a related problem was repo · d recently by Chung et al. [9]. In the experiment, a steel shell free at the top edge and soldered to a disc at the bottom was tested. The fluid gap was provided by using a thick concrete shell as the outer cylinder and the fluid is water. A series of tests was made for four different fluid gap sizes: 2.616 cm (1.03 in.), 1.367 cm (0.538 in.), 0.643 cm (0.253 in.), and 0.384 cm (0.151 in.).

The analytical and experimental results are given in Fig. 8. The general behavior of the theoretical fluid damping is similar to the experimental data. Quantitatively, the agreement is good for circumferential wave number n = 5 and 6 and small gaps, and fair for large gaps. However, the experimental values for n = 4 are much larger than the analytical results. One of the reasons for the discrepancy is attributed to the boundary conditions; the theoretical model is assumed to be simply supported at both ends while the shell tested is fixed at the bottom and free at the top. Since the theoretical and experimental models have different boundary conditions, and the added mass and viscous damping depend on vibrational mode shape, the two models are not expected to give identical results. Another reason is probably associated with the difficulty in determining the damping ratio for a system with high modal de··'ty.

In a similar study for tubes vibrating in a viscous fluid annulus, the analytical results based on the linear viscous theory are in good agreement with the experimental results for damping and added mass [7]. Since the same theory is used here, as long as the motion is small, the analytical results based on the linear viscous theory are expected to be reliable.

V. CONCLUDING REMARKS

In this paper, an analysis is presented for coupled vibrations of two concentric shells separated by a viscous fluid. The coupling effects are accounted for using fluid stress coefficient matrix of concentric shells. With this analysis, natural frequencies and modal damping of coupled concentric shells in viscous fluid can readily be obtained.

In the analysis the three-dimensional, linearized, Navier-Stokes equations governing the motion of viscous fluids are used. The displacements of the shells are assumed to be small such that the equations of state and motion can be linearized. The analytical results are in reasonable agreement with the published experimental data.

Numerical results are presented for a few selected problems for an incompressible fluid. It is shown that the fluid stress coefficient is always a decreasing function of α_1, Mo_1, Re_1 and r_2/r_1 and in most cases it will decrease as n increases. The sensitivity of Re_1 on $Re\{\alpha_{pq}\}$ is much smaller than that on $Im\{\alpha_{pq}\}$. For general cases, the magnitude of $Re\{\alpha_{pq}\}$ is larger than the magnitude of $Im\{\alpha_{pq}\}$; however when Re_1 is sufficiently small, the magnitude of $Im\{\alpha_{pq}\}$ could be much larger than that of $Re\{\alpha_{pq}\}$ and the damping ratio of the system can therefore be very large.

The lowest natural frequency of the coupled shell system with fluid is significantly lower than those of the individual shells. The frequencies for the first coupled modes (out-of-phase modes) are lower than either of the uncoupled natural frequencies. The effect of the fluid viscosity on the system natural frequencies is negligibly small in most practical systems. However, the modal damping ratio is noticeably increased for some cases when the fluid viscosity is included, especially for the lower

frequency cases. For a coupled shell system the viscous effects are mostly pronounced for the out-of-phase modes, but these effects are considered to be negligible for the in-phase mode.

Finally, it should be pointed out that results from scaled models, frequently used in practices for design evaluation, may not be conservative if the vibration Reynolds number is not simulated. If the gap is small, or the fluid viscosity is relatively high, the simulation of the vibration Reynolds number Re_1 should be included to ensure that modal damping of the model is properly accounted for.

ACKNOWLEDGMENTS

This work was performed under the sponsorship of the Division of Reactor Development and Demonstration, U. S. Energy Research and Development Administration.

The authors wish to express their gratitude to Dr. M. W. Wambsganss for his constructive comments and continued strong support and encouragement.

REFERENCES

1. S. S. Chen and G. S. Rosenberg, "Dynamics of a Coupled Shell-Fluid System," Nucl. Eng. and Design 32, 304-310 (1975).
2. D. Krajcinovic, "Vibrations of Two Coaxial Cylindrical Shells Containing Fluid," Nucl. Eng. and Design 30, 242-248 (1974).
3. L. Levin and D. Milan, "Coupled Breathing Vibrations of Two Thin Cylindrical Coaxial Shells in a Fluid," Proc. Vibration Problems in Industry, Paper No. 616 (1973), Keswick, England.
4. M. K. Au-Yang, "Free Vibration of Fluid-Coupled Coaxial Cylindrical Shells of Different Lengths," ASME Paper No. 76-WA/APM-3 (1976).
5. W. Flügge, "Stresses in Shells, Springer-Verlag, Berlin (1960).
6. L. D. Landau and E. M. Lifshitz, Fluid Mechanics, Addison-Wesley Publishing Co. Inc., Mass. (1959).
7. S. S. Chen, M. W. Wambsganss, and J. A. Jendrzejczyk, "Added Mass and Damping of a Vibrating Rod in Confined Viscous Fluids," Journal of Applied Mechanics, Transactions of the ASME 43 (Ser. E, Number 2), 325-329 (1976).
8. R. R. Miller, "The Effects of Frequency and Amplitude of Oscillation on the Hydrodynamic Masses of Irregular Shaped Bodies," MS Thesis, University of Rhode Island (1965).
9. H. Chung, P. Turula, T. M. Mulcahy, and J. A. Jendrzejczyk, "Analysis of a Cylindrical Shell Vibrating in a Cylindrical Fluid Region," ANL-76-48 (1976).

APPENDIX

(1) Matrix a_{pq}

$$a_{11} = -\alpha_1 F_n(\gamma_1), \qquad a_{12} = -\alpha_1 G_n(\gamma_1), \qquad a_{13} = a_{14} = 0,$$

$$a_{15} = -\beta_1 F_n(\beta_1), \qquad a_{16} = -\beta_1 G_n(\beta_1), \qquad a_{21} = -n F_n(\gamma_1),$$

$$a_{22} = -n G_n(\gamma_1), \qquad a_{23} = \beta_1 F_{n+1}(\beta_1) - n F_n(\beta_1),$$

$$a_{24} = \beta_1 G_{n+1}(\beta_1) - n G_n(\beta_1), \qquad a_{25} = a_{35} = \alpha_1 F_{n+1}(\beta_1),$$

$$a_{26} = a_{36} = \alpha_1 G_{n+1}(\beta_1) \qquad a_{31} = nF_n(\gamma_1) - \gamma_1 F_{n+1}(\gamma_1),$$

$$a_{32} = n G_n(\gamma_1) - \gamma_1 G_{n+1}(\gamma_1) \qquad a_{33} = n F_n(\beta_1)$$

$$a_{34} = n G_n(\beta_1) \quad \text{and} \quad \alpha_i = k r_i, \quad \beta_i = k_2 r_i, \quad \gamma_i = k_1 r_i \quad .$$

The expression of a_{pq} for p = 4,5,6 is similar to those for p = 1,2,3 and can be obtained by replacing α_1, β_1, and γ_1 by α_2, β_2, and γ_2.

(2) Matrix h_{pq}

$$h_{11} = 2 S_1 \sigma_1 [F_{n+1}(\gamma_1) - \frac{n}{\gamma_1} F_n(\gamma_1)] \quad ,$$

$$h_{12} = 2 S_1 \sigma_1 [G_{n+1}(\gamma_1) - \frac{n}{\gamma_1} G_n(\gamma_1)] \quad ,$$

$$h_{13} = -\frac{S_2 \sigma_2 n}{\beta_1} F_n(\beta_1) \quad , \qquad h_{14} = -\frac{S_2 \sigma_2 n}{\beta_1} G_n(\beta_1) \quad ,$$

$$h_{15} = -S_2 \{(\sigma_2^2 - 1) F_{n+1}(\beta_1) + \frac{n}{\beta_1} F_n(\beta_1)\} \quad ,$$

$$h_{16} = -S_2 \{(\sigma_2^2 - 1) G_{n+1}(\beta_1) + \frac{n}{\beta_1} G_n(\beta_1)\} \quad ,$$

$$h_{21} = \frac{2 S_1 n}{\gamma_1} [F_{n+1}(\gamma_1) - \frac{n-1}{\gamma_1} F_n(r_1)] \quad ,$$

$$h_{22} = \frac{2S_1{}^n}{\gamma_2}\left[G_{n+1}(\gamma_1) - \frac{n-1}{\gamma_1} G_n(r_1)\right] ,$$

$$h_{23} = -S_2\left\{\left[\frac{2n(n-1)}{\beta_1{}^2} - 1\right]F_n(\beta_1) + \frac{2}{\beta_1} F_{n+1}(\beta_1)\right\} ,$$

$$h_{24} = -S_2\left\{\left[\frac{2n(n-1)}{\beta_1{}^2} - 1\right]G_n(\beta_1) + \frac{2}{\beta_1} G_{n+1}(\beta_1)\right\} ,$$

$$h_{25} = S_2\sigma_2\left[F_n(\beta_1) - \frac{2(n+1)}{\beta_1} F_{n+1}(\beta_1)\right] ,$$

$$h_{26} = S_2\sigma_2\left[G_n(\beta_1) - \frac{2(n+1)}{\beta_1} G_{n+1}(\beta_1)\right] ,$$

$$h_{31} = \left[\frac{2\ S_1 n(n+1)}{\gamma_1{}^2} - \left(2\ S_1 + \frac{1}{1 + i\frac{\omega}{\omega_o}}\right)\right] F_n(\gamma_1) + \frac{2S_1}{\gamma_1} F_{n+1}(\gamma_1) ,$$

$$h_{32} = \left[\frac{2\ S_1 n(n+1)}{\gamma_1{}^2} - \left(2\ S_1 + \frac{1}{1 + i\frac{\omega}{\omega_o}}\right)\right] G_n(\gamma_1) + \frac{2S_1}{\gamma_1} G_{n+1}(\gamma_1) ,$$

$$h_{33} = \frac{2\ S_2 n}{\beta_1}\left[\frac{n-1}{\beta_1} F_n(\beta_1) - F_{n+1}(\beta_1)\right] ,$$

$$h_{34} = \frac{2\ S_2 n}{\beta_1}\left[\frac{n-1}{\beta_1} G_n(\beta_1) - G_{n+1}(\beta_1)\right] ,$$

$$h_{35} = 2\ S_2\sigma_2\left[F_n(\beta_1) - \frac{n+1}{\beta_1} F_{n+1}(\beta_1)\right] ,$$

$$h_{36} = 2\ S_2\sigma_2\left[G_n(\beta_1) - \frac{n+1}{\beta_1} G_{n+1}(\beta_1)\right] ,$$

and $$S_1 = i\frac{\gamma_1{}^2}{Re_1} , \quad S_2 = i\frac{\beta_1{}^2}{Re_1} , \quad \frac{\omega}{\omega_o} = \frac{Mo_1{}^2}{Re_1}\left(\frac{4}{3} + \frac{\nu_o'}{\nu_o}\right) ,$$

$$\sigma_1 = \alpha_1/\gamma_1 , \quad \sigma_2 = \alpha_1/\gamma_2 , \quad Re_1 = \frac{\omega\ r_1{}^2}{\nu_o} , \quad Mo_1 = \frac{\omega\ r_1}{C_o} .$$

Again, the expression of h_{pq} for p = 4,5, and 6 is also omitted here since it is similar to those of p = 1, 2, and 3; they can be obtained by replacing β_1 and γ_1 by β_2 and γ_2, and multiplied by -1 [e.g., $h_{43} = \frac{S_2\sigma_2{}^n}{\beta_2} F_n(\beta_2)$].

(3) Matrix C_{pq}

$$C_{11} = \alpha_1^2 + \frac{1-\nu_1}{2} n^2 \left(1 + \frac{\delta_1^2}{12}\right) ,$$

$$C_{12} = C_{21} = \frac{1+\nu_1}{2} \alpha_1 n ,$$

$$C_{22} = n^2 + \frac{1}{2}(1-\nu_1)\left(1 + \frac{\delta_1^2}{4}\right)\alpha_1^2 ,$$

$$C_{13} = C_{31} = \alpha_1\nu_1 + \frac{\alpha_1^3}{12}\delta_1^2 - \frac{\alpha_1}{24}(1-\nu_1)\delta_1^2 n^2 ,$$

$$C_{23} = C_{32} = n + \frac{\alpha_1^2}{24}(3-\nu_1)\delta_1^2 n ,$$

$$C_{33} = 1 + \frac{\delta_1^2}{12}\left[1 - 2n^2 + (\alpha_1^2 + n^2)^2\right] ,$$

$$\delta_i = h_i/R_i .$$

The expression of C_{pq} for the outer shell can be obtained easily by replacing α_1 and δ_1 by α_2 and δ_2 and changing the subscript for C_{pq} from 1, 2, and 3 to 4, 5, and 6 respectively.

LIST OF ILLUSTRATIONS

Fig. No.	Title
1	Schematic of two concentric cylindrical shells containing a viscous fluid.
2	Stress coefficient α_{33} as a function of Reynolds number Re_1 for $\alpha_1 = \pi$, $r_2/r_1 = 1.1$ and $Mo_1 = 0.0$.
3	Real parts of stress coefficients as functions of radius ratio r_2/r_1 for $\alpha_1 = \pi$ and $Mo_1 = 0.0$. ———: $Re\{\alpha_{66}\}$; - - - - -: $Re\{\alpha_{33}\}$.
4	Imaginary parts of stress coefficients as functions of r_2/r_1 for $\alpha_1 = \pi$ and $Mo_1 = 0.0$. ———: $Im\{-\alpha_{66}\}$; - - - - - - -: $Im\{-\alpha_{33}\}$.
5	Natural frequencies of shell systems.
6	Modal damping ratio ζ of a fluid/shell system.
7	Modal shape of a coupled fluid/shell system.
8	Comparison of experimental and analytical damping ratio.

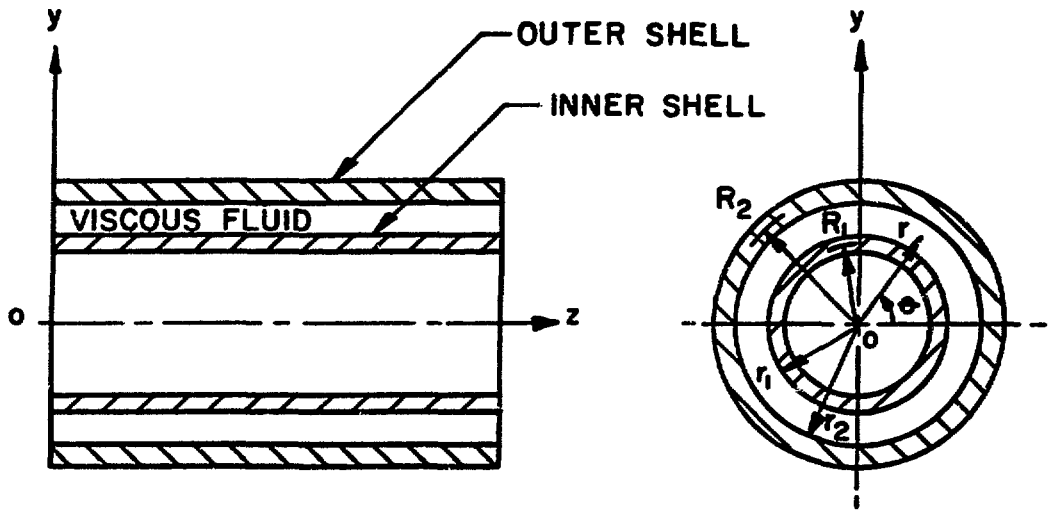

Fig. 1. Schematic of two concentric cylindrical shells containing a viscous fluid.

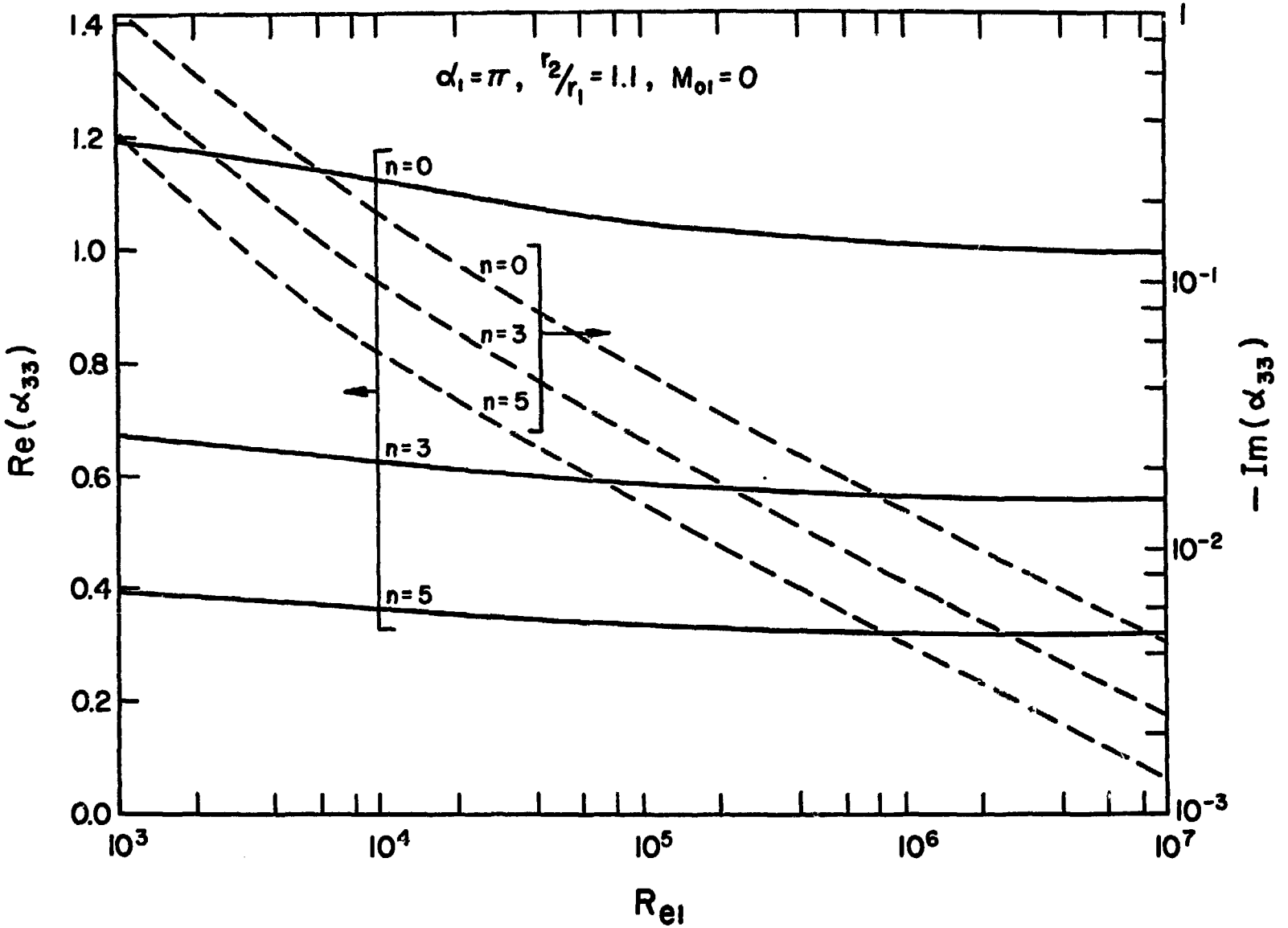

Fig. 2. Stress coefficient α_{33} as a function of Reynolds number Re_1 for $\alpha_1 = \pi$, $r_2/r_1 = 1.1$, and $Mo_1 = 0.0$.

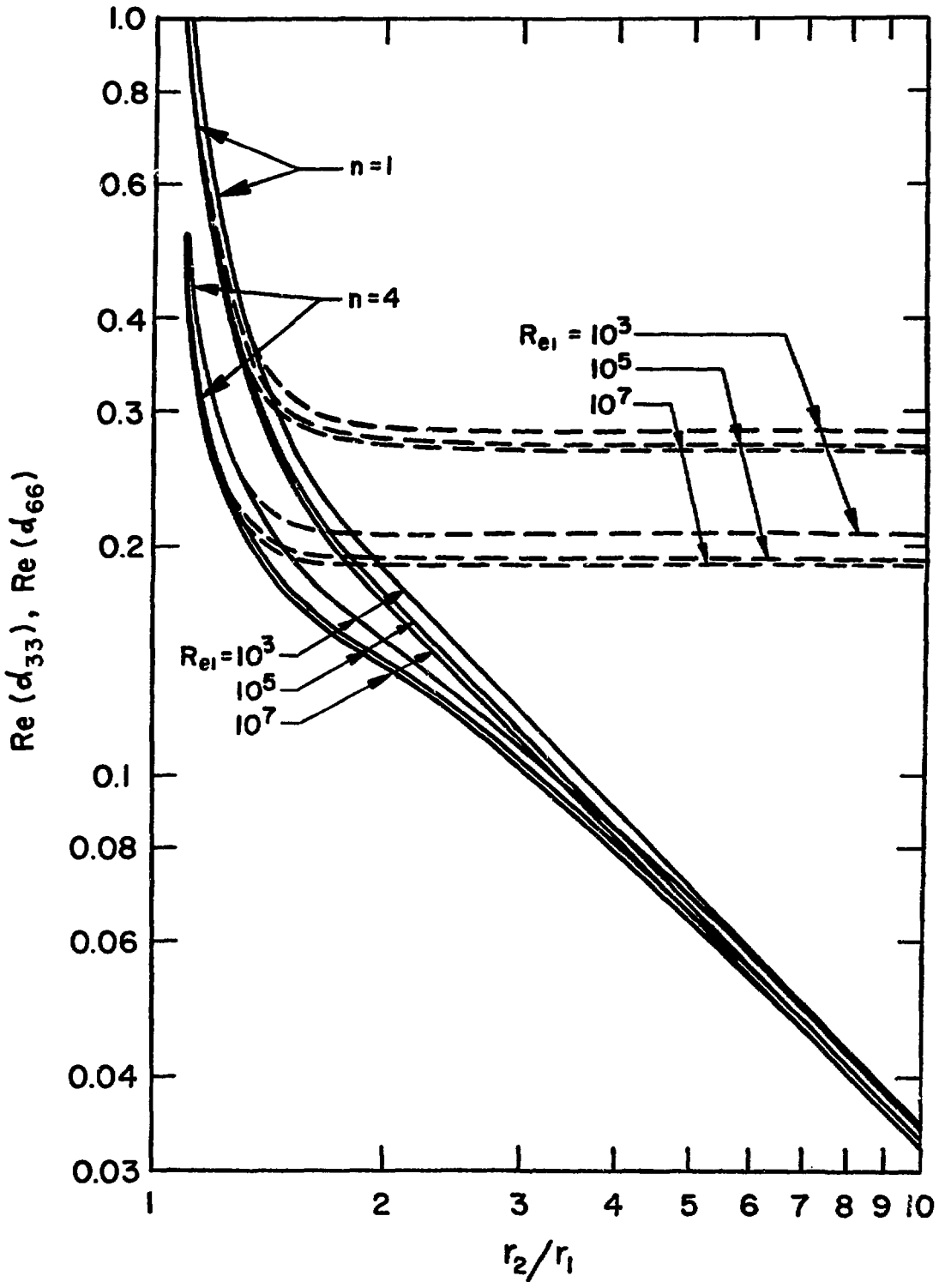

Fig. 3. Real parts of stress coefficients as functions of radius ratio r_2/r_1 for $\alpha_1 = \pi$ and $Mo_1 = 0.0$. ————: $Re\{\alpha_{66}\}$; – – – – –: $Re\{\alpha_{33}\}$.

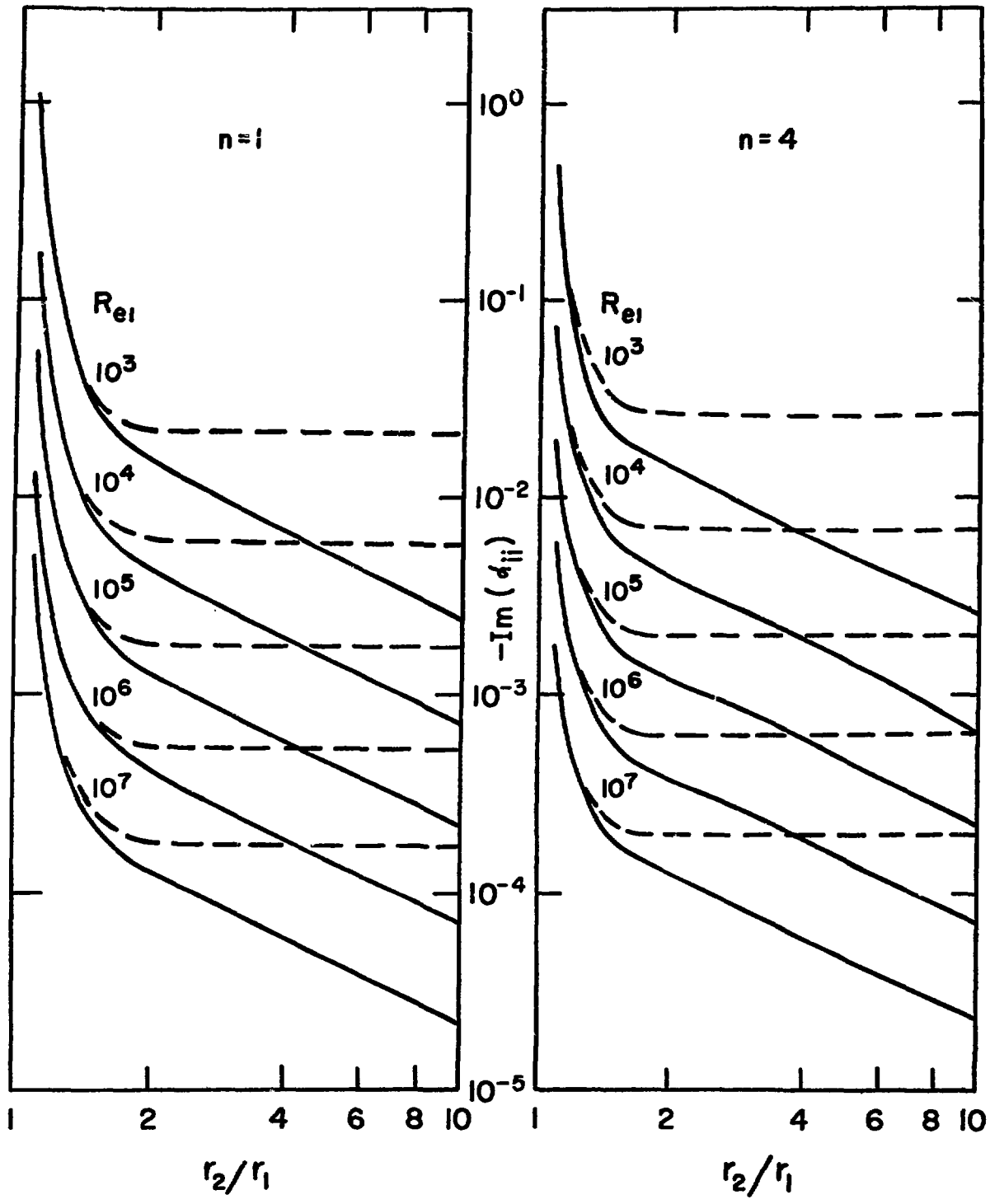

Fig. 4. Imaginary parts of stress coefficients as functions of r_2/r_1 for $\alpha_1 = \pi$ and $Mo_1 = 0.0$. ————: $Im\{-\alpha_{66}\}$; – – – – –: $Im\{-\alpha_{33}\}$.

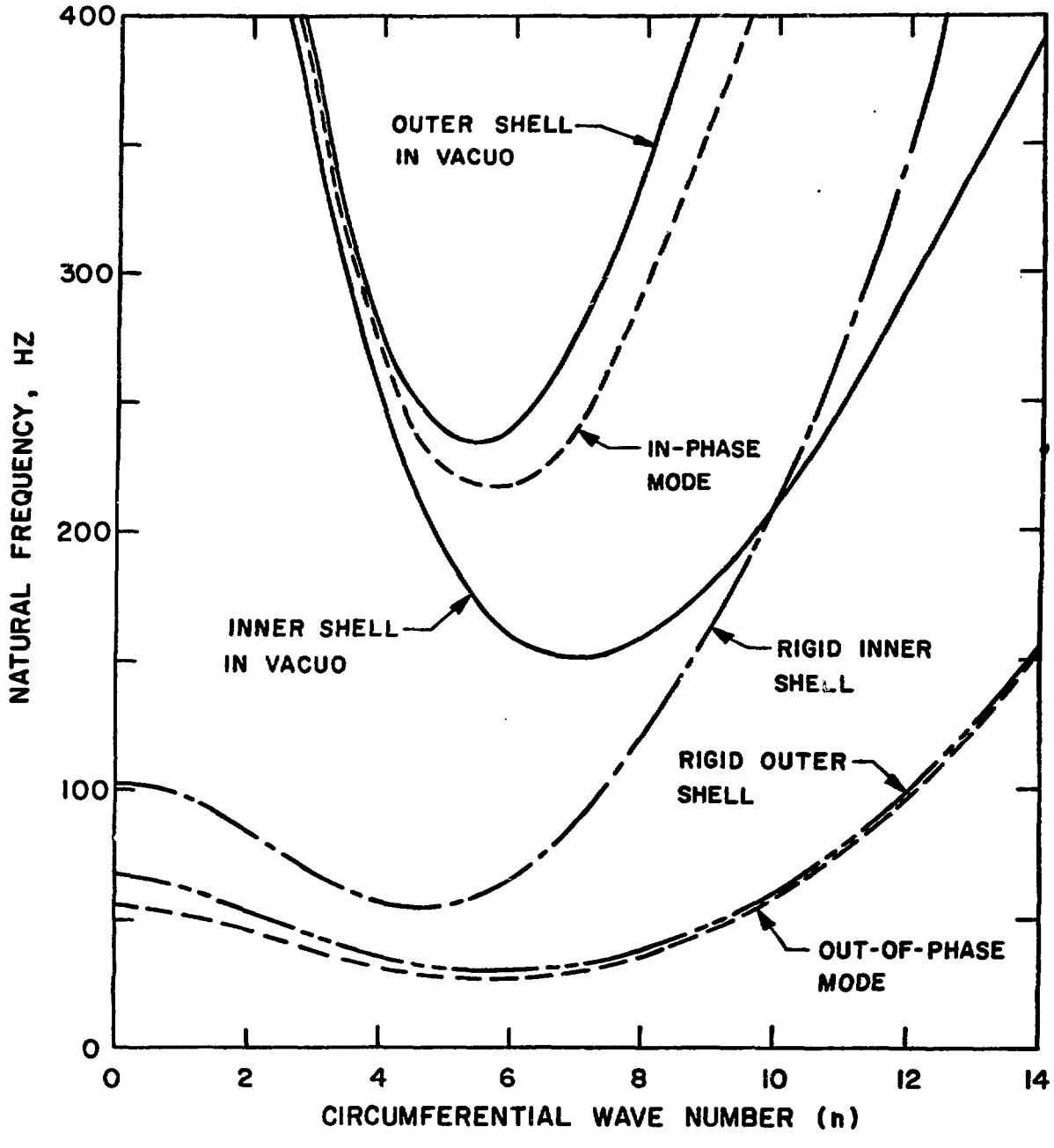

Fig. 5. Natural frequencies of shell systems.

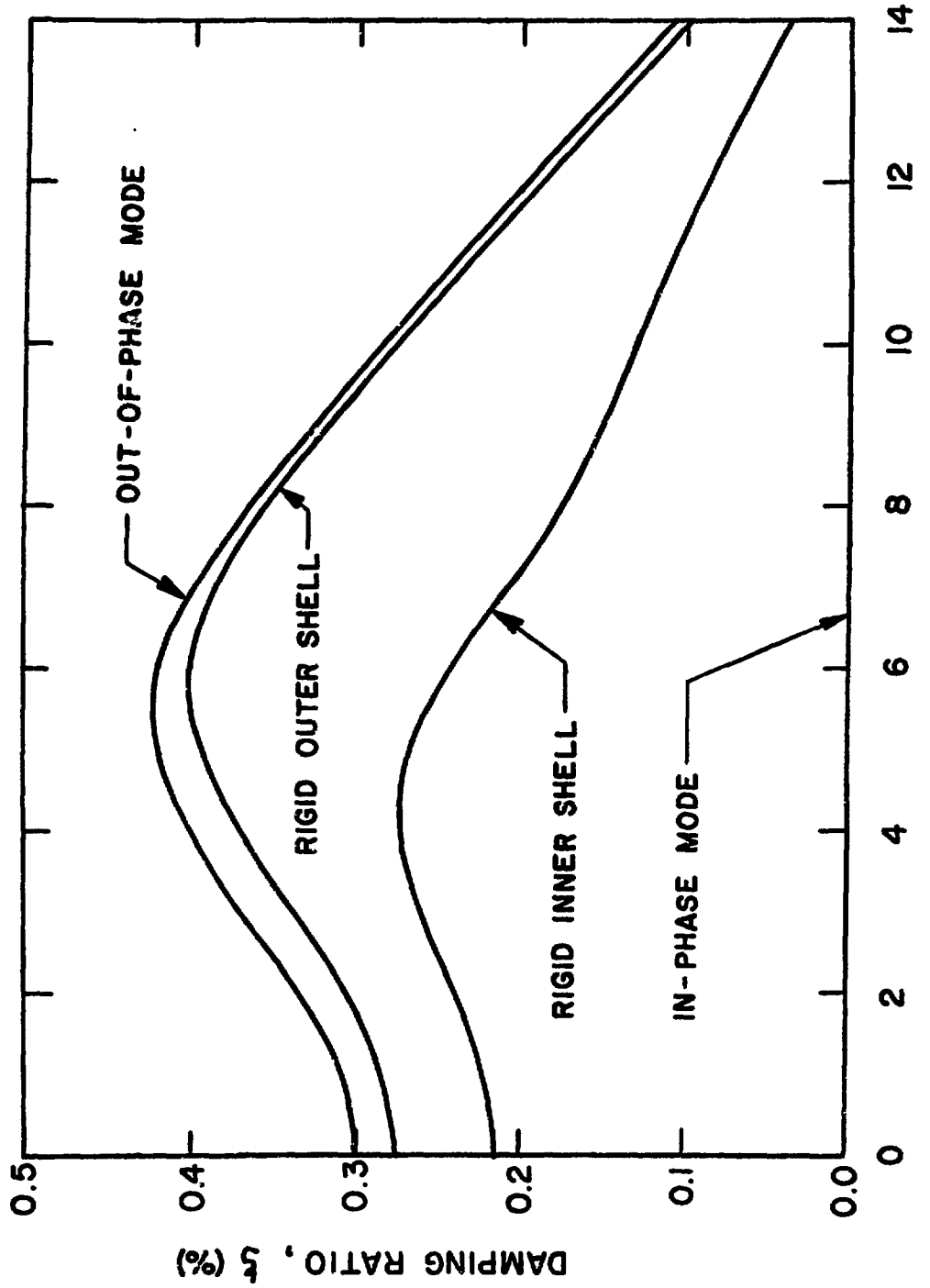

Fig. 6. Modal damping ratio ζ of a fluid/shell system.

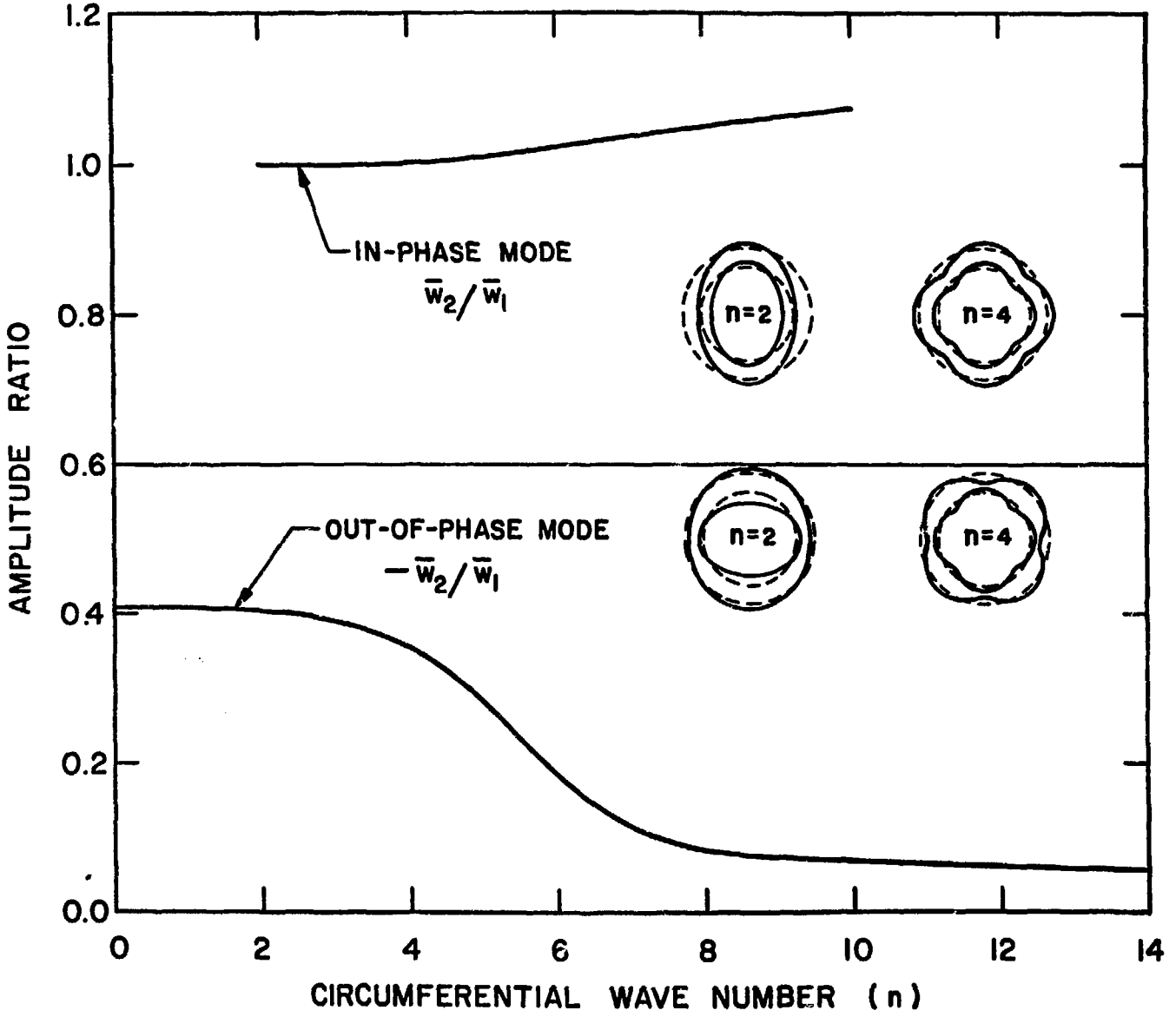

Fig. 7. Modal shape of a coupled fluid/shell system.

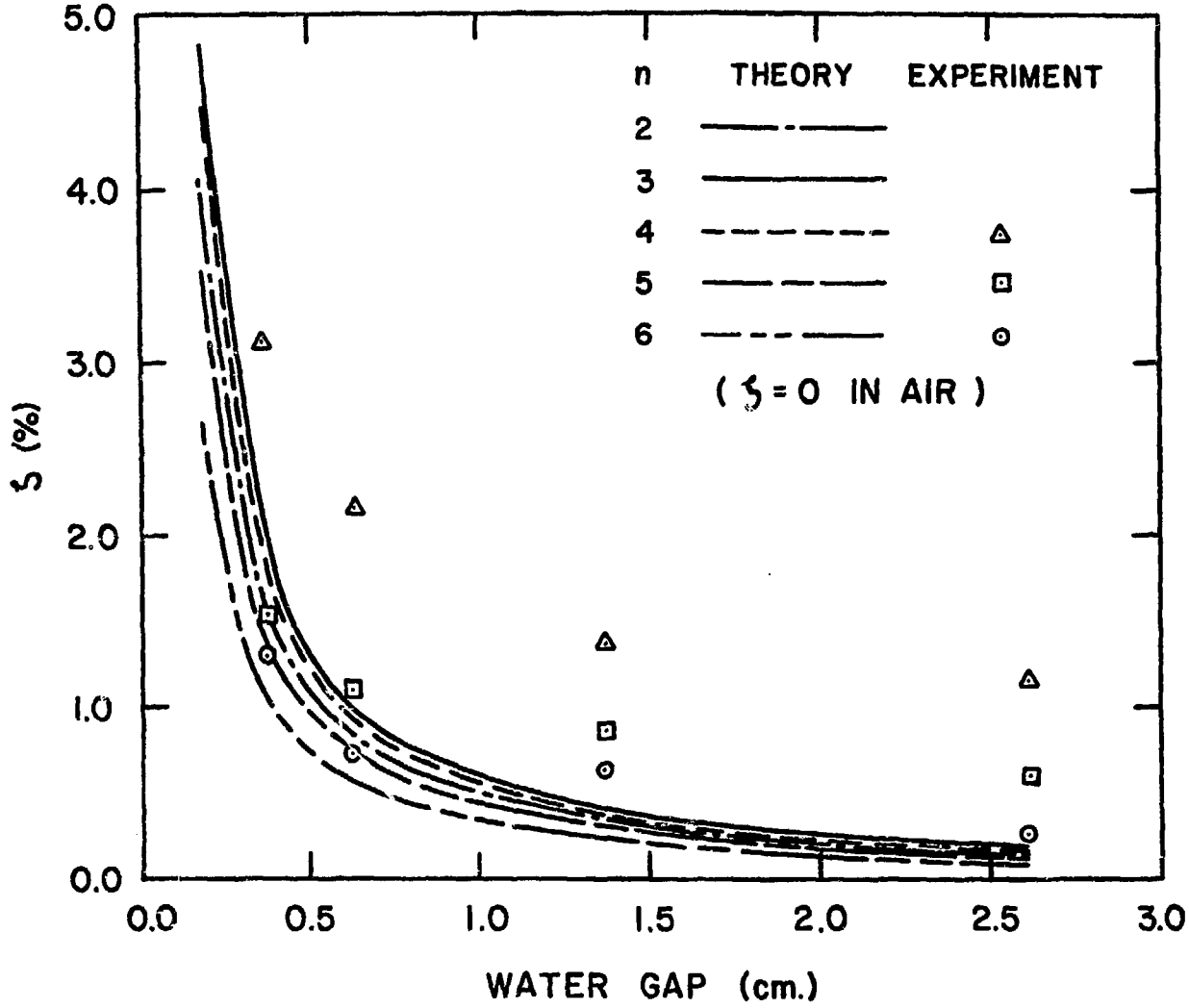

Fig. 8. Comparison of experimental and analytical damping ratio.